Research Paper
Bone Biology

Osteoconductive effectiveness of bone graft derived from antler cancellous bone: an experimental study in the rabbit mandible defect model

X. Zhang[1,2], Q. Cai[3], H. Liu[4], B. C. Heng[5], H. Peng[1], Y. Song[2], Z. Yang[2], X. Deng[1]

[1]Department of Geriatric Dentistry, Peking University School and Hospital of Stomatology, Beijing, PR China; [2]College of Animal Science and Veterinary Medicine, Jilin University, Changchun, Jilin, PR China; [3]Key Laboratory of Carbon Fiber and Functional Polymers, Ministry of Education, Beijing University of Chemical Technology, Beijing, PR China; [4]Department of Materials Science and Engineering, Tsinghua University, Beijing, PR China; [5]ETH-Zurich, Department of Biosystems Science & Engineering, Basel, Switzerland

Abstract. The purpose of this study was to evaluate the properties of a novel inorganic xenogenic bone substitute, calcinated antler cancellous bone (CACB). Physicochemical properties of CACB including surface morphology, phase composition, chemical bond structure, Ca/P ratio and porosity were characterized by scanning electron microscopy, X-ray diffraction spectroscopy, Fourier-transform infrared spectroscopy, inductively coupled plasma-atomic emission spectroscopy and nitrogen adsorption analysis, and were found to closely resemble calcinated human cancellous bone. The bone defect repair efficacy of CACB was evaluated in comparison with commercially available bone substitutes (Bio-Oss®) within rabbit mandible defects. The gross observation, micro-CT and histology analysis data demonstrated that CACB was efficacious for bone regeneration, and was comparable with Bio-Oss® bone substitute in inducing neovascularization and osteogenesis within the mandible defects. CACB can therefore serve as a safe, renewable, and sustainable source of bone graft material, but without the ethical issues pertaining to animal welfare.

Bone graft implantation is a major treatment modality for bone deficiencies arising from various diseases, traumas and congenital defects, with effective clinical outcomes being reported.[1–3] Although autologous bone graft is considered the gold standard in clinical practice, extensive research effort is focused on synthetic materials to avoid the problems of limited availability, additional surgery, and potential donor site morbidity associated with autologous bone grafts.[4,5] The clinical application of artificial bone substitutes is uncommon and utilized for only a narrow range of indications because of their uncertain clinical efficacy and lack of osteoinductive properties.[6] Xenogenic grafts are among the most common materials utilized clinically owing to their ready availability and good osteoconductivity as a result of their origin from natural bone tissues of animals,[7,8] examples are Bio-Oss®[9–11]

or Endobon[®12] derived from bovine femur, and OsteoBiol[®13] derived from porcine bone.

Although the clinical performance of these inorganic xenografts bone substitutes has been confirmed and widely accepted by physicians and patients,[9,11] the disadvantage of these products are their high price, the time-consuming manufacturing process, and controversial ethical issues pertaining to animal slaughter.[14–16] Therefore, a safe, effective, sustainable and ethically acceptable bone graft substitute material would be of substantial clinical interest.

Antlers are the only body parts that can achieve complete regeneration in mammals, and are one of the fastest growing tissues, with a peak growth rate of 2–4 cm every day.[17] This extraordinary growth rate is the result of the rich blood supply arising from the highly vascularized velvet tissue on the antler surface, and from the pedicle at the antler base.[17,18] Every year, deer antlers begin to grow in spring (March–April), mature after 3–4 months of growth, and are naturally shed, to conserve energy, at the end of the autumn mating season. This cycle is repeated annually.[19] The remarkable growth rate and material properties of antler make it an interesting model for bone growth and regeneration.[20] Much interest is focused on the structural and mechanical properties of antler arising from their main function as the shield and weapon during mating combat.[21,22] Little is known about the clinical efficacy of utilizing antler as a bone xenograft substitute for bone defect repair.

Antlerogenesis involves rapid deposition of calcium and phosphate in a short period of time, resulting in the formation of a cancellous bone-like structure in the central portions of antlers.[23] Antlers have a similar composition to human cancellous bones and other mammalian long bones,[17] but differ substantially from keratin-based mammalian horns.[24] The authors hypothesize that calcinated antler cancellous bone (CACB) may serve as an ethically acceptable xenograft substitute for bone defect repair. In this study, the cancellous portions of naturally shed Sika deer antlers were calcinated at 800 °C for 6 h. The composition and physiochemical properties of CACB were rigorously characterized. The efficacy of CACB in promoting bone defect repair in situ in rabbit mandibles was evaluated compared with inorganic bone substitutes (Bio-Oss[®]) that are used clinically.

Materials and methods

Naturally-shed antlers from adult male Sika deer (*Cervus nippon*) were purchased from Jilin Wilderness Trading Company (Changchun, China). The commercially available Bio-Oss[®] bone substitute was supplied by Switzerland Geistlich-Pharma, Co., Ltd. Human cancellous bone (gamma-irradiated and freeze-dried vertebral bone; Batch No. 3460285/2009) was kindly provided by Ao Rui Biological Material Co., Ltd. (Shanxi, China). Sodium hydroxide, chloroform methanol and hydrogen peroxide were obtained from Sigma-Aldrich Inc. (St. Louis, MO, USA).

Preparation and characterization of CACB

The cancellous portion of naturally-shed and fresh antlers was obtained by removing the cortex (Fig. 1A and B). To eliminate organic components of the bone blocks, chemical treatment and high temperature calcination were carried out as previously described.[25] Briefly, the cancellous bone blocks were immersed in 2% (w/v) sodium hydroxide for 12 h, and then in 30% hydrogen peroxide for 24 h; followed by washing in flowing tap water. The pieces were immersed in a 3:1 mixture of chloroform and methanol for 1 h and dried at 70 °C for 24 h. The pieces were sintered at 800 °C over a period of 6 h and maintained at that temperature for 3 h in a tube-type furnace to obtain CACB. The bone blocks were milled and sieved to obtain similar sized granules as the control
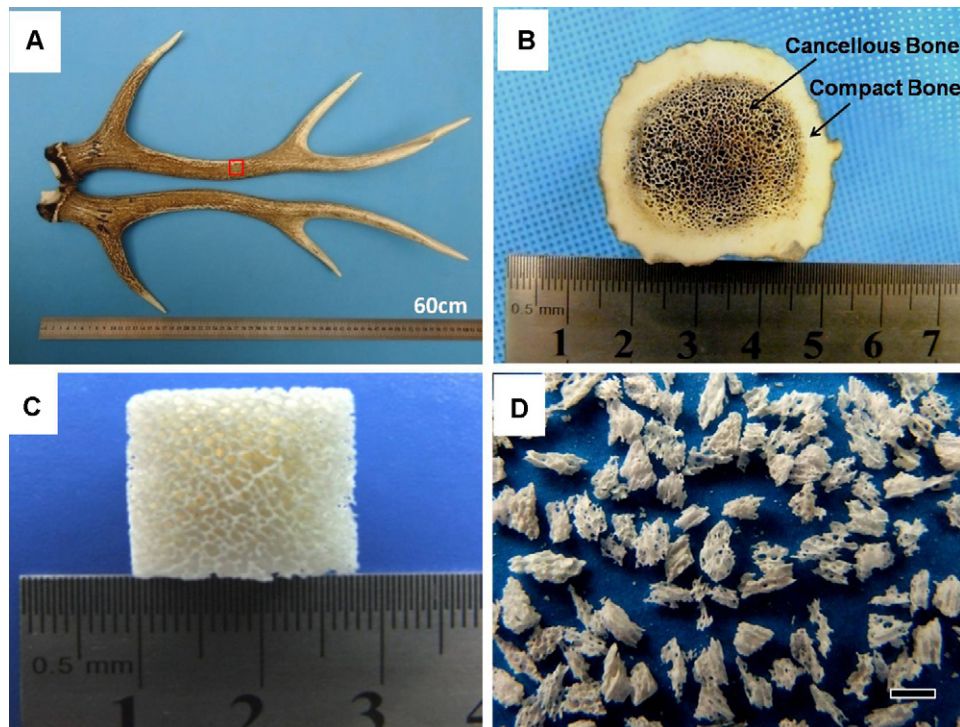

Fig. 1. Naturally shed Sika deer antlers (about 60 cm in length) (A), cross-section of antler (B), macroscopic image of CACB cube (C) and granules (D) after removal of proteins and lipids, and calcination.

material (Bio-Oss®) with diameter ranging between 1.0 and 2.0 mm (Fig. 1D).

The surface morphology and structure of the bone blocks were characterized using scanning electron microscopy (SEM; ZEISS, Supra 55, Germany). The phase composition and chemical bond structure of bone blocks were evaluated by X-ray diffraction spectroscopy (XRD, Rigaku D/max 2500 VB2+/PC, Japan) and Fourier-transform infrared spectroscopy (FT-IR, Nicolet 8700, USA). Inductively coupled plasma-atomic emission spectroscopy (ICP-AES, SPS8000, Thermo Elemental, USA) was used to analyze the Ca/P ratio of the CACB. The porosity was determined with nitrogen adsorption (brunauer–emmet–teller; BET isotherm) using a Sorpty 1750 (Carlo Erba) apparatus. For these analyses, the calcinated human cancellous bone was calcinated by the same method as that of CACB, and was used as a control.

Experimental animals and surgical procedures

All animal experiments were performed in accordance with a protocol approved by the Laboratory Animal Care and Use Committee of Peking University. 18 healthy New Zealand white rabbits weighting approximately 3.0 kg each were evenly divided into three groups: CACB group; Bio-Oss® group; and untreated group. The surgical procedure for creating experimental mandible defects was performed according to a previously published protocol.[26] The rabbits were anesthetized with pentobarbital sodium (1 mg/kg). After shaving the skin and disinfecting the surgical site in each animal, a parallel skin incision was made along the inferior border of the mandible on both sides. After exposing the masseter muscle, subperiosteal elevation of the muscle's detachment was performed buccally and lingually, exposing the bone of the jaw angle. Under continuous saline irrigation, a slowly rotating trephine burr was used to create circular defects 8 mm in diameter in the region anterior to the jaw angles on every side of the mandible of each rabbit (Fig. 2). A diameter of 5 mm in this experimental model has been reported to correspond to the critical size that prevents spontaneous healing during an animal's lifetime.[27] Each defect was flushed with saline to remove bone debris and then implanted with 0.25 g of either CACB or Bio-Oss® granules. The experimental defect was left completely untreated (untreated group) as a control. Each treatment was randomly applied to each defect in a rabbit. The mucoperiosteal flaps were carefully sutured over the defect area using 3-0 absorbable sutures. After surgery, each rabbit received an intramuscular injection of sodium ampicillin at a dose of 20,000 U/kg every day for 3 successive days. Animals were killed by lethal intravenous administration of sodium pentobarbital at specific time points (4 and 12 weeks after the transplantation) for tissue processing.

Micro-CT analysis

12 weeks post-surgery, the animals were killed and their mandibles were explanted and fixed in 10% neutral buffered formalin. The mandible defect site was assessed by gross observation, and the morphology of the reconstructed mandibles was assessed using a micro-CT system (Skyscan 1076; Skyscan, Aartselaar, Belgium). The CT settings were: X-ray energy levels at 70 kV, current at 139 µA, and integration time of 600 ms with 300 projections per 180°. After scanning, the reconstructed data were segmented using a threshold algorithm as reported previously,[20] and a three-dimensional (3D) histomorphometric analysis was performed automatically (three independent regions in each group). The parameters of bone mineral densities (BMD) and bone volume fraction (bone volume/total volume, BV/TV) were used for comparison in this study.

Histological evaluation

All the rabbit mandibles from the three groups after 4 and 12 weeks post-surgery were subjected to tissue processing and sectioning as reported previously.[28,29] Briefly, the tissue samples were fixed in 10% neutral buffered formalin for 7 days, followed by decalcification and dehydration, and finally embedded in paraffin and sectioned at 5 µm thickness. Haematoxylin–eosin (H–E) and Masson's trichrome staining were performed separately on consecutive tissue sections, and images were captured under microscopy (CX21, Olympus, Japan).

Statistical analysis

Quantitative data were presented as mean ± standard deviation (SD). Statistical differences between groups were evaluated by Student's *t*-test using the software SPSS 13.0 (SPSS Science). A *p*-value < 0.05 was considered statistically significant.

Results

Physicochemical characterization of CACB

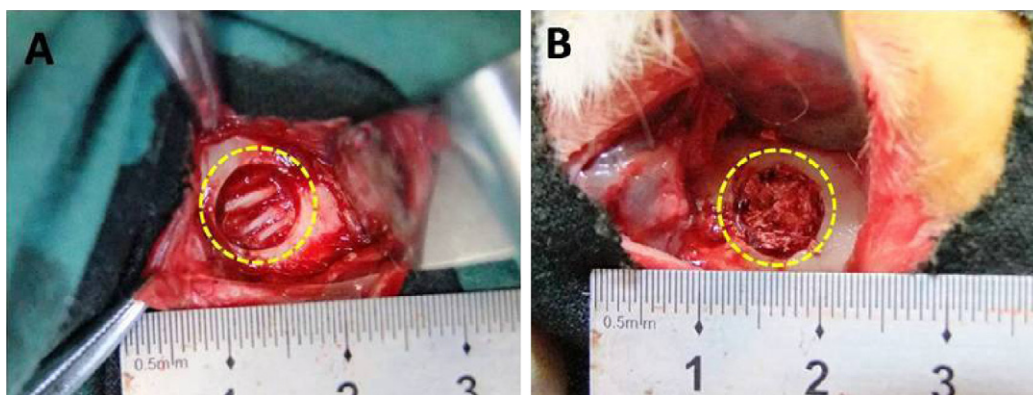SEM images of the surface morphology and microstructure of CACB compared

Fig. 2. Illustration of surgical procedure. (A) Bone defects of 8 mm in diameter created on the region anterior to the jaw angles of rabbit mandible (yellow dashed line circle). (B) Defect filled with CACB or Bio-Oss® granules. (For interpretation of the references to color in this figure legend, the reader is referred to the web version of the article.)
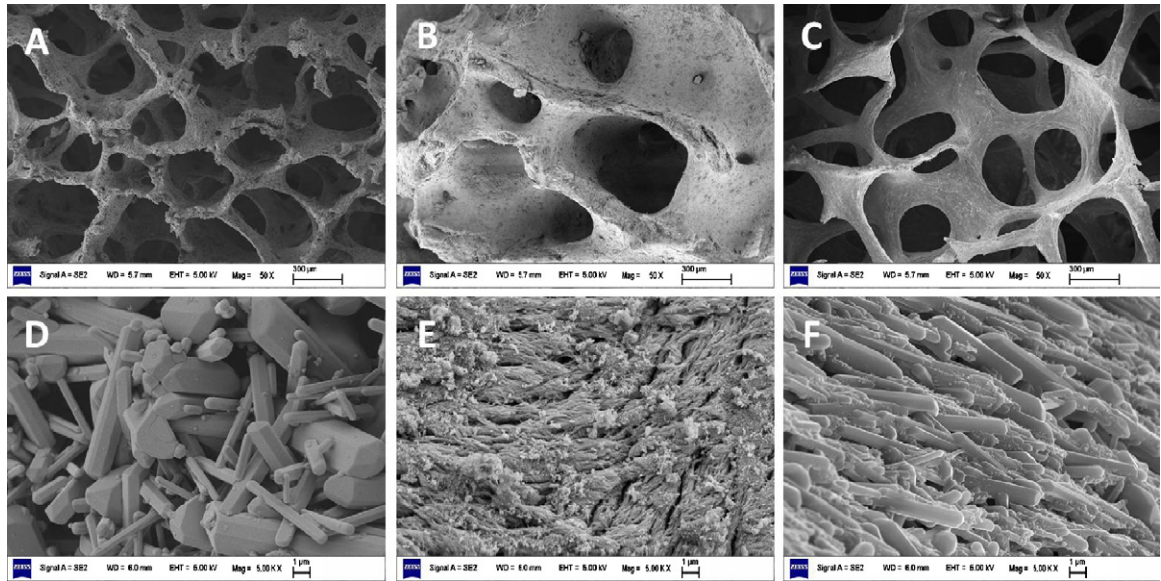
Fig. 3. SEM images of calcinated bone of different natural origins. (A and D) CACB derived from antlers, (B and E) Bio-Oss® derived from femur of calf and (C and F) human cancellous bone.

Table 1. Physicochemical properties of CACB, Bio-Oss®, and calcinated human cancellous bone.

Specimen	CACB	Bio-Oss®	Calcinated human cancellous bone
Pore size (μm)	300–600	200–500	300–800
Porosity (%)	75 ± 2.23	71 ± 4.35	79 ± 3.14
Ca/P ratio	1.81	1.47	1.76

with Bio-Oss® and calcinated human cancellous bone are shown in Fig. 3. CACB exhibited a highly porous and well-interconnected pore structure. The pore size range of CACB was typically around 300–600 μm, which was in a similar scale to that of calcinated human cancellous bone (300–800 μm) and Bio-Oss® (200–500 μm) (Table 1). The volumetric porosity of CACB was 75 ± 2.23%, which was comparable to the corresponding values of 79 ± 3.14% and 71 ± 4.35%

obtained for calcinated human cancellous bone and Bio-Oss®, respectively. The higher magnification SEM imaging revealed that CACB possessed hexagonal apatite crystal morphology, which more closely resembled calcinated human cancellous bone, compared to Bio-Oss®. The XRD spectrograph demonstrated that the characteristic peaks of CACB corresponded to the characteristic peaks of hydroxyapatite (HA) and that of calcinated human cancellous bone (Fig. 4A).

Additionally, CACB more closely resembled the crystal structure of calcinated human cancellous bone apatite minerals compared to Bio-Oss®. The FT-IR spectrograph confirmed that the composition of CACB was mainly carbonated hydroxyapatite (Fig. 2B) with the Ca/P ratio of CACB being 1.81 (Table 1). All these features were similar to those of calcinated human cancellous bone, suggesting that CACB would be a suitable matrix for bone regeneration.

Micro-CT measurement

To assess the 3D structure of the repaired mandible, micro-CT images were taken at 12 weeks post-surgery. In the CACB group, it was found that the boundary between the mandible defect site and surrounding host bone was indistinguishable
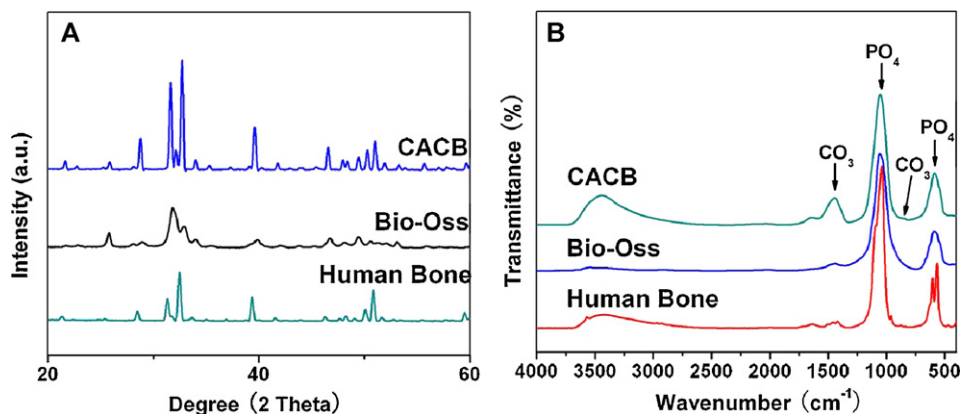

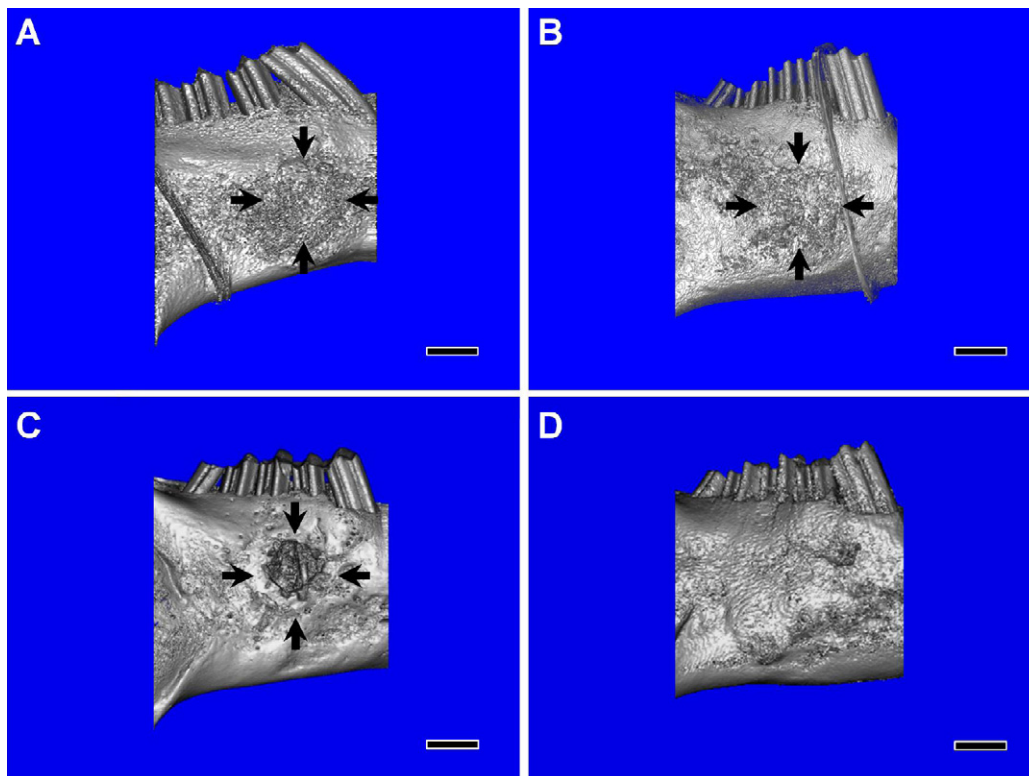*Fig. 4*. XRD (A) and FT-IR (B) spectrograph of CACB, Bio-Oss® and calcinated human cancellous bone.

Fig. 5. Micro-CT images of mandibular bony defects taken 12 weeks after implantation. (A) CACB group, (B) Bio-Oss® group, (C) untreated group and (D) normal mandible. Scale bar: 4 mm. Black arrows denote the surgical site.

(Fig. 5A), which is similar to the Bio-Oss® group (Fig. 5B). The regenerated bone tissue at the defect site was flushed with the surrounding host bone and the surface morphology of the healed mandible closely resembled that of normal mandible (Fig. 5D), suggesting that desirable repair of the defect area has been achieved. In the untreated group, the mandible defect site was left largely unrepaired and remained a conspicuous introcession (Fig. 5C).

To quantify calcification within the repaired mandible, local BMD of implants in the CACB and Bio-Oss® group were assessed by micro-CT analysis at 12 weeks post-surgery. As shown in Fig. 6A, the CACB group showed relatively high BMD of (541.10 ± 26.76) mg HA/cm^3, {} which was similar to that of the Bio-Oss® group (561.17 ± 22.30) mg HA/cm^3 and the normal mandible (594.34 ± 20.42) mg HA/cm^3. By contrast, in the untreated group, the local BMD at the defect site without any implant was (213.50 ± 25.59) mg HA/cm^3, which was significantly lower than that of the CACB group ($p < 0.05$) and the Bio-Oss® group ($p < 0.05$). The ratio BV/TV, as an indicator of the relative amount of newly formed bone, was significantly higher for the CACB group when compared to the untreated group (Fig. 6B), but was similar for both the CACB and Bio-Oss® groups. These results confirmed that both the CACB and Bio-Oss® scaffolds displayed similar levels of osteogenesis upon implantation.

Histological results

At 4-weeks post-implantation, the boundary between the defect area and host bone could still be clearly identified. H–E staining revealed that a large amount of small blood vessels and some osteoblasts were observed around both the CACB and Bio-Oss® implants. This is clear evidence of neovascularization and formation of neonatal bone (Fig. 7A and B). Masson staining showed that the fibrous tissue surrounding the implants was mainly composed of newly formed and regularly aligned collagen fibres that were stained green (Fig. 7D and E). By contrast, numerous haematoma filled the defect area in the untreated group (Fig. 7C). Masson staining showed that there were numerous red-stained blood clots and little green-stained collagen fibres (Fig. 7F).

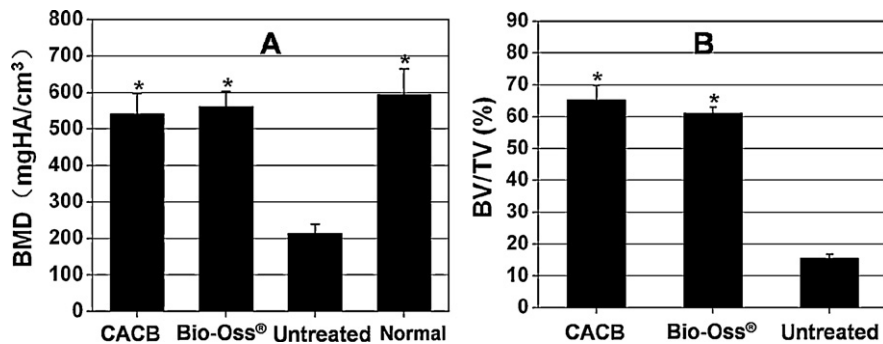At 12-weeks post-implantation, it was observed that for both the CACB group

Fig. 6. Quantitative analysis of bone defect repair at 12 weeks after implantation with CACB, Bio-Oss® or no graft filling (untreated). (A) Bone mineral density (BMD) and (B) bone volume/tissue volume (BV/TV). *$p < 0.05$ with respect to untreated group.
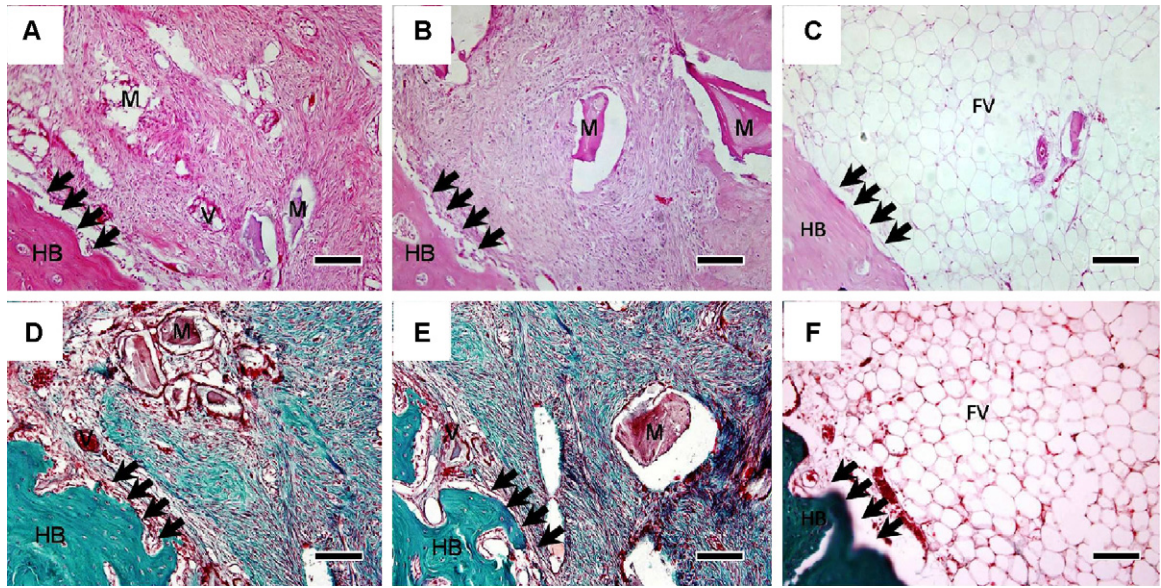
Fig. 7. Histological analysis of bone formation 4 weeks after implantation. (A–C) Representative histological analysis (H–E staining) of bone formation 4 weeks after implantation of CACB (A), Bio-Oss® (B), and untreated groups (C). (D–F) Representative histological analysis (Masson staining) of bone formation 4 weeks after implantation of the CACB (D), Bio-Oss® (E), and untreated groups (F). Black arrows denote the boundary between nascent bone and host bone. M, materials; NB, nascent bone; HB, host bone; V, vessels; FV, fat vacuoles. Scale bar: 200 μm.
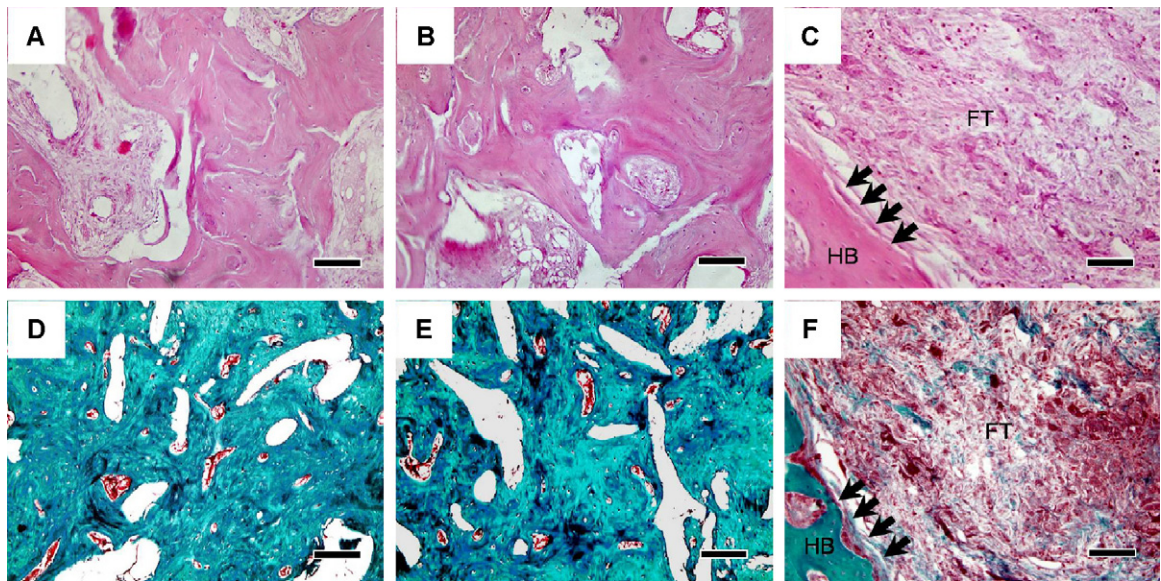

Fig. 8. Histological analysis of bone formation 12 weeks after implantation. (A–C) Representative histological analysis (H–E staining) of bone formation 12 weeks after implantation of the CACB (A), Bio-Oss® (B), and untreated groups (C). (D–F) Representative histological analysis (Masson staining) of bone formation 12 weeks after implantation of CACB (D), Bio-Oss® (E), and untreated groups (F). Black arrows denote the boundary between nascent bone and host bone. HB, host bone; FT, fibrous tissue. Scale bar: 200 μm.

and Bio-Oss® group, the interface between neonatal bone and host bone was indistinguishable due to the mature bone structures having filled the bone defect region (Fig. 8A and B). Masson staining showed that the original green-stained collagen fibres were replaced by mature woven bone in the central bone defect region (Fig. 8D and E). By contrast, in the untreated group, the defects exhibited no tendency of recovery but were filled with fibrous tissues (Fig. 8C and F). As confirmed by gross morphology (Fig. 9A and B), the rabbit mandible defects healed well and the nascent bone was indistinguishable from the host bone after 12 weeks implantation of CACB and Bio-Oss®, while the defect exhibited no signs of recovery in the untreated group and remained a conspicuous introcession after detaching the filled fibrous tissues (Fig. 9C).

Discussion

Bone graft implantation is a major treatment modality for bone defect repair and reconstruction.[5] Various inorganic xenogenic bone substitutes have been studied and their clinical use has been approved

Fig. 9. Macroscopic photographs of mandible defects 12 weeks after implantation. (A) CACB group, (B) Bio-Oss® group and (C) untreated group. Scale bar: 10 mm. Black arrows denote the surgical site.

due to their extensive availability and acceptable efficacy in repairing and healing bone defects.[7–9,25,30] Host animals must be slaughtered to obtain xenogenic graft material and this leads to animal ethics and welfare issues.[14–16] In this study, naturally-shed antlers were evaluated as an ethically acceptable xenograft substitute for bone defect repair. The findings of this study showed that CACB had similar physicochemical properties to calcinated human cancellous bone, including phase composition, chemical bond structure, Ca/P ratio, pore size and porosity. This supports the application of CACB as a safe, renewable, and sustainable source of bone graft material, but without ethical issues pertaining to animal welfare.

In the field of bone defect repair, it is critical to select appropriate filling materials.[31] An ideal bone graft material should provide space for infiltrating cells to attach, proliferate, and produce new extracellular matrix.[6] Pore size and porosity of the materials play a critical role in bone formation.[32,33] Previous studies showed that pore sizes > 300 μm and porosity ranging from 70 to 80% are optimal for enhanced vascularization and osteogenesis, due to appropriate exchange and supply of oxygen and nutrients.[33,34] In this study, the pore size (300–600 μm) and porosity (75 ± 2.23%) of CACB were similar to those of calcinated human cancellous bone. Therefore, the results suggest that CACB might be an appropriate candidate for bone defect repair.

The XRD data demonstrated that the characteristic peaks of CACB closely corresponded to that of hydroxyapatite and calcinated human cancellous bone. Previous reports showed that antlers had very similar composition to human cancellous bones and long bones of other mammalian species such as pig[10] and cattle,[35] but differ substantially from keratin-based mammalian horns.[24] Antler also had structural similarity to calcinated cancellous bones of ostrich tibia.[25] FT-IR spectrograph data confirmed that the composition of CACB was mainly carbonated hydroxyapatite. This was similar to the results obtained with calcinated human cancellous bone in this study, as well as with previous reports that the chemical composition of Bio-Oss® was mainly carbonated hydroxyapatite.[36] ICP-AES analysis demonstrated that the Ca/P ratio of CACB was 1.81, which was similar to the ratio of calcinated human cancellous bone. All these properties implied that CACB could be preferable for bone defect repair.

When a defect is above a critical size, a template or scaffold is required to guide bone repair. For mandibular defects within the rabbit model, around 5 mm in diameter is generally regarded as the appropriate critical size for evaluating bone graft materials.[37,38] In this study, a bone defect of 8 mm diameter was created in the mandible of rabbits for implantation with either CACB or Bio-Oss®. The micro-CT analysis and gross morphology of mandible samples at 12 weeks post-surgery showed that the mandible defects in both the CACB group and Bio-Oss® group demonstrated good healing, whereas the untreated group exhibited no signs of recovery and remained a conspicuous introcession.

It is likely that the composition and structure of Bio-Oss® is similar to that of human cancellous bone, which provides an optimal microenvironment for bone ingrowth.[36] In this study, CACB also resembled the features of calcinated human cancellous bone in morphology, pore size and structure, chemical composition and crystalline structure. After 4 weeks post-implantation, histological analysis showed that abundant small blood vessels had formed in the area implanted with CACB, indicating occurrence of neovascularization (Fig. 7A).

Masson staining showed that numerous newly formed and regularly aligned collagen fibres were observed surrounding the implants, which implied active osteogenesis (Fig. 7D). At 12 weeks post-implantation, the original green-stained collagen fibres had been replaced by mature woven bone filling in the central bone defect region (Fig. 8A and D). The bone regeneration process induced by CACB was similar to that induced by Bio-Oss®.

Typically, this started from bone-forming cells secreting bone matrix (i.e. collagen) into the defect area, followed by mineralization to envelope the implanted graft material.[39] As fusion and integration of the implanted materials with the surrounding bone tissue occurred, bone defect healing was completed.[40] Kim et al.[41] reported similar results with a bioactive cancellous bone graft derived from pig by a heat-treatment method; it exhibited excellent osteoconductive effectiveness for tibia defect repair in beagle dogs due to its ideal chemical and structural characteristics. More recently, Sawada et al.[25] reported an ostrich cancellous bone derived substitute with pore sizes 200–500 μm and average porosity of about 70% resulting in successful bone regeneration of calvarial defects in rabbits. Owing to the excellent physicochemical properties of CACB as shown by the results of this study, CACB is therefore a promising biomaterial for clinical application in the repair of bone defects. Ready accessibility of CACB for use without ethical issues pertaining to animal slaughter would make it appealing to both patients and clinicians.

Funding

Competing interests

None declared.

Ethical approval

The Laboratory Animal Care and Use Committee of Peking University approved all procedures in this study.

References

1. Hesse E, Kluge G, Atfi A, Correa D, Haasper C, Berding G, et al. Repair of a segmental long bone defect in human by implantation of a novel multiple disc graft. *Bone* 2010;**46**:1457–63.

2. Parikh SN. Bone graft substitutes in modern orthopedics. *Orthopedics* 2002;**25**:1301–9.

3. Torroni A. Engineered bone grafts and bone flaps for maxillofacial defects: state of the art. *J Oral Maxillofac Surg* 2009;**67**:1121–7.

4. Jiang XQ, Zhao J, Wang SY, Sun XJ, Zhang XL, Chen J, et al. Mandibular repair in rats with premineralized silk scaffolds and BMP-2-modified bMSCs. *Biomaterials* 2009;**30**:4522–12.

5. Petite H, Viateau V, Bensaid W, Meunier A, de Pollak C, Bourguignon M, et al. Tissue-engineered bone regeneration. *Nat Biotechnol* 2000;**18**:959–63.

6. Hollister SJ. Porous scaffold design for tissue engineering. *Nat Mater* 2005;**4**:518–24.

7. Develioglu H, Saraydin SU, Kartal U. The bone-healing effect of a xenograft in a rat calvarial defect model. *Dent Mater J* 2009;**28**:396–400.

8. Develioglu H, Saraydin SU, Kartal U, Taner L. Evaluation of the long-term results of rat cranial bone repair using a particular xenograft. *J Oral Implantol* 2010;**36**:167–74.

9. Carmagnola D, Adriaens P, Berglundh T. Healing of human extraction sockets filled with Bio-Oss®. *Clin Oral Implants Res* 2003;**14**:137–43.

10. Shin JW, Park SA, Yang YI, Kim YK, Park KD, Lee JW, et al. In vitro study of osteogenic differentiation of bone marrow stromal cells on heat-treated porcine trabecular bone blocks. *Biomaterials* 2004;**25**:527–35.

11. Zitzmann NU, Scharer P, Marinello CP, Schupbach P, Berglundh T. Alveolar ridge augmentation with Bio-Oss®: a histologic study in humans. *Int J Periodontics Restorative Dent* 2001;**21**:289–95.

12. Briem D, Linhart WL, Lehmann W, Meenen NM, Rueger JM. Long-term results after application of a porous hydroxyapatite ceramic (Endobon) in proximal tibia fractures. *Unfallchirurg* 2002;**105**:128–33.

13. Figueiredo M, Henriques J, Martins G, Guerra F, Judas F, Figueiredo H. Physicochemical characterization of biomaterials commonly used in dentistry as bone substitutes—comparison with human bone. *J Biomed Mater Res B* 2010;**92B**:409–19.

14. Amirfeyz R, Stanley D. Allograft-prosthesis composite reconstruction for the management of failed elbow replacement with massive structural bone loss: a medium-term follow-up. *J Bone Joint Surg Br* 2011;**93**:1382–8.

15. Mellor DJ, Littin KE. Using science to support ethical decisions promoting humane livestock slaughter and vertebrate pest control. *Anim Welf* 2004;**13**:S127–32.

16. Yang YG, Sykes M. Xenotransplantation: current status and a perspective on the future. *Nat Rev Immunol* 2007;**7**:519–31.

17. Chen PY, Stokes AG, McKittrick J. Comparison of the structure and mechanical properties of bovine femur bone and antler of the North American elk (Cervus elaphus canadensis). *Acta Biomater* 2009;**5**:693–706.

18. Antlers HJ. Bones of contention. *Nature* 1969;**224**:1036–7.

19. Antlers HJ. Unbrittle bones of contention. *Nature* 1971;**231**:469.

20. Jones AC, Arns CH, Hutmacher DW, Milthorpe BK, Sheppard AP, Knackstedt MA. The correlation of pore morphology, interconnectivity and physical properties of 3Dceramic scaffolds with bone in growth. *Biomaterials* 2009;**30**:1440–51.

21. Landete-Castilleijos T, Currey JD, Estevez JA, Gaspar-Lopez E, Garcia A, Gallego L. Influence of physiological effort of growth and chemical composition on antler bone mechanical properties. *Bone* 2007;**41**:794–803.

22. Launey ME, Chen PY, McKittrick J, Ritchie RO. Mechanistic aspects of the fracture toughness of elk antler bone. *Acta Biomater* 2010;**6**:1505–14.

23. Gyurjan I, Borsy A, Molnar A, Steger V, Szabolcsi Z, Orosz L. Initiation of bone formation during antler development. *Bone* 2006;**39**:S26.

24. Searl M. Horns or antlers—which is which. *Sierra* 1983;**68**:96–7.

25. Morita S, Sawada Y, Hokugo A, Yang YW, Kamitani M, Matsuda S, et al. A novel hydroxyapatite ceramic bone substitute transformed by ostrich cancellous bone: characterization and evaluations of bone regeneration activity. *J Biomed Mater Res B* 2011;**98B**:217–22.

26. Thomaidis V, Kazakos K, Lyras DN, Dimitrakopoulos I, Lazaridis N, Karakasis D, et al. Comparative study of 5 different membranes for guided bone regeneration of rabbit mandibular defects beyond critical size. *Med Sci Monit* 2008;**14**:BR67–73.

27. Schmitz JP, Hollinger JO. The critical size defect as an experimental model for craniomandibulofacial nonunions. *Clin Orthop Relat Res* 1986;**205**:299–308.

28. Guo H, Su J, Wei J, Kong H, Liu C. Biocompatibility and osteogenicity of degradable Ca-deficient hydroxyapatite scaffolds from calcium phosphate cement for bone tissue engineering. *Acta Biomater* 2009;**5**:268–78.

29. Ren T, Ren J, Jia X, Pan K. The bone formation in vitro and mandibular defect repair using PLGA porous scaffolds. *J Biomed Mater Res A* 2005;**74**:562–9.

30. Stavropoulos A, Karring T. Guided tissue regeneration combined with a deproteinized bovine bone mineral (Bio-Oss®) in the treatment of intrabony periodontal defects: 6-year results from a randomized-controlled clinical trial. *J Clin Periodontol* 2010;**37**:200–10.

31. Bohner M. Resorbable biomaterials as bone graft substitutes. *Mater Today* 2010;**13**:24–30.

32. Griffith LG, Swartz MA. Capturing complex 3D tissue physiology in vitro. *Nat Rev Mol Cell Biol* 2006;**7**:211–24.

33. Karageorgiou V, Kaplan D. Porosity of 3D biomaterial scaffolds and osteogenesis. *Biomaterials* 2005;**26**:5474–91.

34. Kasten P, Beyen I, Niemeyer P, Luginbuhl R, Bohner M, Richter W. Porosity and pore size of beta-tricalcium phosphate scaffold can influence protein production and osteogenic differentiation of human mesenchymal stem cells: an in vitro and in vivo study. *Acta Biomater* 2008;**4**:1904–15.

35. Epple M, Tadic D. A thorough physicochemical characterisation of 14 calcium phosphate-based bone substitution materials in comparison to natural bone. *Biomaterials* 2004;**25**:987–94.

36. Benke D, Olah A, Mohler H. Protein-chemical analysis of Bio-Oss bone substitute and evidence on its carbonate content. *Biomaterials* 2001;**22**:1005–12.

37. Andersson L, Ramzi A, Joseph B. Studies on dentin grafts to bone defects in rabbit tibia and mandible; development of an experimental model. *Dent Traumatol* 2009;**25**:78–83.

38. He H, Huang JQ, Ping FY, Sun G, Chen GF. Calcium alginate film used for guided bone regeneration in mandible defects in a rabbit model. *Cranio* 2008;**26**:65–70.

39. Nudelman F, Pieterse K, George A, Bomans PHH, Friedrich H, Brylka LJ, et al. The role of collagen in bone apatite formation in the presence of hydroxyapatite nucleation inhibitors. *Nat Mater* 2010;**9**:1004–9.

40. Abushahba F, Renvert S, Polyzois I, Claffey N. Effect of grafting materials on osseointegration of dental implants surrounded by circumferential bone defects—an experimental study in the dog. *Clin Oral Implants Res* 2008;**19**:329–34.

41. Kim SH, Shin JW, Park SA, Kim YK, Park MS, Mok JM, et al. Chemical, structural properties, and osteoconductive effectiveness of bone block derived from porcine cancellous bone. *J Biomed Mater Res B* 2004;**68B**:69–74.

Address:
Xuliang Deng
Department of Geriatric Dentistry
Peking University School and Hospital
  of Stomatology
Beijing 100081
PR China
Tel: +86 10 82195637;
Fax: +86 10 82195581
E-mail: kqdengxuliang@bjmu.edu.cn